Control and Performance Analysis of a Reconfigurable Multi-Copter

Robert Niemiec
PhD Student
Rensselaer Polytechnic Institute, Troy, New York

Farhan Gandhi
Redfern Chair Professor
Rensselaer Polytechnic Institute, Troy, New York

Rajneesh Singh
Vehicle Analysis Team Lead, Vehicle Technology Directorate
US Army Research Lab, Aberdeen Proving Grounds, Maryland

ABSTRACT

This paper presents a concept of a multi-copter that can be reconfigured between a quadcopter, hexacopter, octocopter and decacopter. The maximum useful weights of the octocopter, hexacopter and quadcopter, were 77%, 55% and 32% that of the decacopter. The controls for each of the configurations are identified and for the configurations with control redundancy, the power optimal controls are presented. A dynamic simulation model is implemented and used to compare the various configurations. Over a range of aircraft useful weights, it was observed that the decacopter required minimum power when the useful weight was greater than around 30% of its maximum, due to lower induced and profile power requirements of the lighter loaded slower spinning rotors. At lower useful weights, the hexacopter required less power due to its significantly lower empty weight. The octocopter and quadcopter did not emerge as low-power configurations of choice. Increasing the number of rotors increased the maximum hover endurance. At a useful weight corresponding to 53% of the decacopter's maximum useful weight, the decacopter's hover endurance time was 9% higher than that of the hexacopter. At low useful weights, the maximum pitch and yaw accelerations generated by the hexacopter were around 80-95% higher than the decacopter, but at higher useful weights the decacopter's accelerations were around 60% higher. All multi-copter configurations displayed a longitudinal and lateral phugoid mode in hover. Compared to the hexacopter, the phugoid modes for the decacopter had significantly higher components of surge rate compared to pitch rate, or sway rate compared to roll rate, while the modal damping ratios were 20-40% lower.

INTRODUCTION

In recent years there has been a growing interest in vertical lift based on distributed electric propulsion. In addition to the reduction in weight and complexity possible by eschewing mechanical drivetrains, distributed electric propulsion offers tremendous flexibility in optimally integrating propulsion into the airframe as needed. Distributed electric propulsion is most commonly found on classical multi-copters (quadcopters, hexacopters, octocopters, etc.), but there has also been a flurry of innovative design and development activity focusing on a more comprehensive integration of the propulsion around the airframe. Examples of such efforts include NASA's GL-10 Greased Lightning aircraft (Ref. 1), various designs by Joby Aviation (Refs. 2, 3), and Aurora Flight Sciences' hybrid electric Lightning Strike aircraft (Ref. 4). Other VTOL aircraft designs based on distributed electric propulsion are being pursued by E-Volo, EHang, A^3, Zee.Aero and Lilium Aviation (Ref. 5, 6).

Presented at the AHS International 73rd Annual Forum & Technology Display, Fort Worth, Texas, USA, May 9-11, 2017.

Another significant advantage distributed electric propulsion offers over conventional systems using mechanical drivetrains is the possibility for easy reconfiguration. The Boeing Company recently explored a modular electric vertical lift system (Ref. 7). Combining a number of base units, larger multi-copters could be assembled as required by the mission.

Expanding on the idea of modular vertical lift, the present study focuses on a family of reconfigurable multi-copters, ranging from a quadcopter to a decacopter. The controls for the various configurations within a unified framework are defined, and the power-optimal controls for each configuration are identified. Through simulation, the capabilities and performance of the various configurations are compared, and physical explanations provided for observations made.

MULTI-COPTER CONFIGURATIONS

Figure 1 shows a schematic representation of the quadcopter used as the baseline in this study. As with any quadcopter, adjacent rotors spin in opposite directions. On Fig. 1, rotors 1 and 3 (in blue) are shown spinning in the counter-clockwise (CCW) direction, while rotors 2 and 4 (in red) spin in the clockwise (CW) direction. All the rotors are

connected to a central hub, with an "F" marked on the hub to indicate the front of the aircraft. Also indicated on the figure are the azimuthal coordinates with $\psi = 0°$ toward the tail of the aircraft, $\psi = 90°$ toward the starboard side, $\psi = 180°$ toward the front, and $\psi = 270°$ toward the port side. Unlike a classical quadcopter with an equal azimuthal spacing of 90° between all rotors, the azimuthal spacing between the two rear rotors (3 and 4) is 60°, and the same is true of the spacing between the two front rotors (1 and 2). Thus, as seen in Fig. 1, rotors 1, 2, 3 and 4 are situated at $\psi = 150°$, 210°, 330°, and 30°, respectively, for the baseline quadcopter

The addition of two opposite-spinning rotors (5 and 6), attached directly to the hub (at $\psi = 270°$ and $\psi = 90°$, respectively) as shown in Fig. 2, converts the aircraft to a hexacopter (see picture of hardware in Fig. 3). The initial unequal azimuthal spacing of rotors in the quadcopter configuration was selected such that the rotors now all have equal azimuthal spacing in the hexacopter configuration. Even so, the hexacopter in Fig. 2 differs from a classical hexacopter in that adjacent rotors do not spin in opposite directions.

To accommodate an even larger increase in gross-weight capability, the quadcopter can be extended to an octocopter, instead of a hexacopter. In that case, four rotors can be attached at the ends of the booms of the baseline quadcopter, as shown in Fig. 4, instead of attaching two rotors directly to the hub as done for the hexacopter in Figs. 2 and 3. In this "extended boom" octocopter configuration, the additional rotors (5, 6, 7, and 8) form an outer perimeter and alternate in spin-direction just as the inner perimeter rotors do (see Fig. 4). Finally, the aircraft can be further extended to a decacopter (Fig. 5) by simply reattaching two rotors (9 and 10) directly to the hub of the extended boom octocopter at $\psi = 270°$ and $\psi = 90°$, respectively. As with the hexacopter, the two additional rotors attached to the hub spin in opposite directions, and it is easy to observe that the extension from the octocopter to the decacopter configuration is similar to that from the quadcopter to the hexacopter.

MULTI-ROTOR CONTROLS

The quadcopter in Fig. 1, fundamentally, has four controls corresponding to the speed of each of its rotors. However, varying the speed of an individual rotor produces a highly coupled response. For example, speeding up the CCW-spinning rotor 1 would increase thrust, as well as produce a nose-up pitching moment, a roll-left moment, and a nose-right yaw moment. Reference 8 discusses how multi-rotor controls, instead, can be used to decouple the quadcopter's response and are used on the baseline quadcopter in this study. The multi-rotor controls (Fig. 6) comprise of *collective RPM control, Ω_0* (Fig. 6a), *yaw control, Ω_Y* (Fig. 6b), *pitch control, Ω_P* (Fig. 6c), and *roll control, Ω_R* (Fig. 6d). Collective RPM control speeds up all the rotors to increase thrust, and produces no moments on the aircraft. Yaw control speeds up the CW rotors (2 and 4) while simultaneously slowing down the CCW rotors (1 and 3) to produce only a nose-left yaw-moment (no pitch or roll). Pitch control speeds up the two aft rotors (3 and 4) while slowing down the two front rotors (1 and 2) to produce only a nose-down pitching moment (no roll or yaw). And roll control speeds up the two right rotors (1 and 4) while slowing down the left rotors (2 and 3) to produce only a roll-left moment (no pitch or yaw). The individual rotor speeds are related to the multi-rotor controls as shown below:

$$\begin{Bmatrix}\Omega_1\\ \Omega_2\\ \Omega_3\\ \Omega_4\end{Bmatrix} = \begin{bmatrix}1 & -\sqrt{3}/2 & +1/2 & -1\\ 1 & -\sqrt{3}/2 & -1/2 & +1\\ 1 & +\sqrt{3}/2 & -1/2 & -1\\ 1 & +\sqrt{3}/2 & +1/2 & +1\end{bmatrix}\begin{Bmatrix}\Omega_0\\ \Omega_P\\ \Omega_R\\ \Omega_Y\end{Bmatrix} \quad (1)$$

Hexacopters, with six rotors, have six controls available (corresponding to the RPM of each of its six rotors). It should be noted that any multi-copter requires only four controls to generate thrust and moments about three axes, so control redundancy exists when the number of rotors is greater than four. Reference 9 identifies the orthogonal multi-rotor controls for a classical hexacopter (with adjacent rotors spinning in opposite directions) and further categorizes them into four primary controls (collective RPM, yaw, pitch and roll) and two redundant controls. However, these do not apply to the non-classical hexacopter configuration in Fig. 2 with its non-alternating pattern of rotor spin-direction. Instead, the hexacopter controls can be based off the quadcopter controls with the front rotors (1 and 2) and the rear rotors (3 and 4) in Fig. 2 using the same multi-rotor controls (Ω_0, Ω_Y, Ω_P, and Ω_R) shown in Fig. 6. The speeds of the auxiliary rotors 5 and 6 can be defined in terms of an auxiliary collective RPM and an auxiliary differential control mode (Ω'_{A0} and Ω'_{AD}, respectively), such that

$$\begin{aligned}\Omega_5 &= \Omega'_{A0} + \Omega'_{AD}\\ \Omega_6 &= \Omega'_{A0} - \Omega'_{AD}\end{aligned} \quad (2)$$

The auxiliary collective RPM mode, Ω'_{A0}, speeds up both rotors 5 and 6 equally to generate additional lift. On the other hand, the auxiliary differential mode, Ω'_{AD}, which speeds CCW-spinning rotor 5 but slows CW-spinning rotor 6 would produce coupled roll and yaw moments. To avoid this coupling, Ω'_{AD} is not used in this study, and only Ω'_{A0}, which controls the lift-share between the original quadcopter rotors and the auxiliary rotors is used. Thus, for the hexacopter, in addition to Eq. 1,

$$\Omega_5 = \Omega_6 = \Omega'_{A0} \quad (3)$$

Advancing from the quadcopter to the octocopter in Fig. 4, the outer perimeter rotors (5, 6, 7, and 8) have similar controls to the quadcopter controls in Fig. 6. The auxiliary

collective RPM control, Ω_{A0}, speeds up rotors 5, 6, 7, and 8 equally; auxiliary yaw control, Ω_{AY}, slows the CCW rotors (5 and 7) while speeding up the CW rotors (6 and 8); auxiliary pitch control, Ω_{AP}, speeds up the aft rotors (7 and 8) while slowing down the front rotors (5 and 6); and auxiliary roll control, Ω_{AR}, speeds up the right rotors (5 and 8) while slowing down the left rotors (6 and 7). Thus, similar to Eq. 1,

$$\begin{Bmatrix}\Omega_5\\ \Omega_6\\ \Omega_7\\ \Omega_8\end{Bmatrix} = \begin{bmatrix}1 & -\sqrt{3}/2 & +1/2 & -1\\ 1 & -\sqrt{3}/2 & -1/2 & +1\\ 1 & +\sqrt{3}/2 & -1/2 & -1\\ 1 & +\sqrt{3}/2 & +1/2 & +1\end{bmatrix}\begin{Bmatrix}\Omega_{A0}\\ \Omega_{AP}\\ \Omega_{AR}\\ \Omega_{AY}\end{Bmatrix} \quad (4)$$

For the octocopter, the auxiliary controls associated with the outer perimeter rotors can be used for lift-share (Ω_{A0}), pitch share (Ω_{AP}), roll share (Ω_{AR}), and yaw share (Ω_{AY}). In other words, control about any axis can be provided by a combination of inner perimeter (quadcopter) controls and outer perimeter (auxiliary) controls. For example, pitching moments can be generated through some combination of Ω_P and Ω_{AP}.

Extending from the octocopter (Fig. 4) to the decacopter (Fig. 5), the octocopter controls described in Eqs. 1 and 4 are preserved, and the rotors 9 and 10 are controlled collectively (while setting differential control mode to zero, as was done for the hexacopter). Thus, for the decacopter,

$$\Omega_9 = \Omega_{10} = \Omega'_{A0} \quad (5)$$

For the decacopter, pitch, roll and yaw moments can be introduced using a combination of Ω_P and Ω_{AP}, Ω_R and Ω_{AR}, and Ω_Y and Ω_{AY}, but lift can be generated using a combination of Ω_0, Ω_{A0} and Ω'_{A0}.

MODELING

To compare the performance of the various multi-copter configurations, as well as the control authority and the autonomous flight dynamic characteristics, a dynamic simulation that can model the quadcopter through the deca-copter configurations is implemented. The accelerations on the aircraft are determined by summing the forces and moments acting about three axes. In addition to gravity and fuselage drag, the forces and moments on each rotor hub are considered. These are obtained using blade-element theory to calculate the elemental aerodynamic loads which are then integrated along the blade span and azimuth and summed over the two blades, for every rotor. The rotor induced velocities are calculated using a 3x4 (10-state) Peters-He dynamic wake model (Ref. 10), applied to each individual rotor. While many models consider simple approximation of rotor thrust and torque, it was noted in Ref. 8 that a proper representation of the inflow over the rotor disk allows an accurate calculation of these quantities, as well as additional rotor hub forces (including pitching moment, side force, etc.). In the present analysis the rotor blades are assumed to be rigid and any interactional aerodynamics between rotors is neglected.

To satisfy force and moment equilibrium about three axes, a trim solution can be determined comprising of four rotor controls along with the aircraft pitch and roll attitude. In the case of the quadcopter where only four rotor controls are available, the trim solution is unique. For all configurations with control redundancy, the redundant controls are parametrically varied to determine the power optimal controls. After identifying these power optimal controls (in terms of RPM ratios for lift share, pitch share, roll share and yaw share), these are used on each multi-copter to compare their hover and forward flight performance, as well as their hover endurance capability.

It should be noted that to compare the maximum moments and accelerations that each configuration can generate, the power optimal controls are not used. In this case, an optimization problem is set up to determine the controls that maximize either the pitch, roll or yaw moment on the aircraft, while the remaining force and moment equilibrium equations are used as constraint equations.

To compare the autonomous flight dynamic characteristics of the various configurations in hover, the nonlinear equations of the aircraft are numerically linearized about their trim condition. With inflow dynamics occurring on a much smaller time scale, the static condensation method is used to reduce the problem size to just the aircraft states (shown to be a viable approach in Ref. 8). The eigen-values and eigen-vectors of this reduced system are then obtained. In particular, this paper compares the behaviors of phugoid modes of the various configurations.

Table 1. Rotor and other aircraft specifications

Parameter	Value
Rotor Radius	12.44 cm
Root Pitch	21.5°
Tip Pitch	11.1°
Root Chord	2.5 cm
Tip Chord	1.0 cm
Quad/Hex Boom Length	30.48 cm
Oct Boom Length	60.96 cm
Motor/Rotor mass	81.6 g each
Boom mass/unit length	1 g/cm
Central hub mass	660g

Specifications for the individual rotor, motor and booms used in the assembly of the various multi-copter configura-tions are provided in Table 1. The airfoil on each rotor blade blends between the NACA 4412 and Clark Y. The central hub mass, and the weight of the appropriate number of rotors/motors and boom sections is used to estimate the aircraft empty weight. The positions of the individual rotor units (based on the schematics in Figs. 1, 2, 4 and 5) are

further considered in estimating the pitch, roll and yaw inertias. Each rotor is assumed to have a minimum operating speed of 2000 RPM and a maximum operating speed of 8000 RPM corresponding to a maximum thrust of 666.67g in hover.

POWER OPTIMAL CONTROLS

The quadcopter in Fig. 1 has only four controls yielding a unique trim solution at any flight condition. For the hexacopter in Fig. 2, a single redundant control, Ω'_{A0} (which determines the speed of rotors 5 and 6), is used as previously discussed. Of the primary controls, hover requires only the use of the *collective RPM control*, Ω_0, with the *yaw, pitch and roll controls* (Ω_Y, Ω_P and Ω_R) all going to zero. The single redundant control, Ω'_{A0}, is parametrically varied, and for a nominal hexacopter gross weight of 2kg, the variation of the collective RPM control and aircraft power requirement is shown in Fig. 7. As Ω'_{A0} increases and rotors 5 and 6 carry more load, the RPM (Ω_0) of rotors 1, 2, 3, and 4 is seen to decrease. The power requirements are seen to be a minimum when $\Omega'_{A0} = \Omega_0$, implying all six rotors operate at the same speed.

As previously noted, the octocopter in Fig. 4 has four redundant controls (Ω_{A0}, Ω_{AY}, Ω_{AP} and Ω_{AR}). In hover, no yaw, pitch, or roll control is required, and it can be shown that the power optimal solution corresponds to $\Omega_{A0} = \Omega_0$. Similar to the hexacopter, for the generation of a required thrust at minimum power, all eight rotors operate at the same speed. When pitch, roll, or yaw control inputs are required, the question of control allocation (share) between the inner and outer rotors arises. For a nominal gross weight of 2.667kg, the auxiliary pitch control, Ω_{AP}, is parametrically varied in Fig. 8 and the pitch control, Ω_P, required to generate a unit pitching moment is calculated and plotted. Also shown on Fig. 8 is the power required as a function of Ω_{AP}. Clearly, as speed Ω_{AP} increases, the requirement on Ω_P decreases. To generate the required pitching moment at minimum power it is observed that $\Omega_{AP} = 2\Omega_P$. Thus, the speed change on the outer perimeter rotors is twice as large as that on the inner perimeter rotors. Similar results (not shown in the paper) were obtained for roll control, and it was noted that $\Omega_{AR} = 2\Omega_R$ to power optimally generate a required roll moment. The factor of 1:2 on inner to outer perimeter rotor speed changes is observed because the outer perimeter rotors are twice the distance from the centroid ($\alpha = 2$). In general, the relationship between speeds of the outer and inner perimeter rotors would be $\Omega_{AP} = \alpha\Omega_P$ and $\Omega_{AR} = \alpha\Omega_R$ for power optimal generation of pitch and roll moments. Next, Fig. 9 shows the yaw control, Ω_Y, required to generate a specified yawing moment (of 0.13 Nm) as the auxiliary yaw control, Ω_{AY}, is parametrically varied. Also shown on Fig. 9 is the corresponding power requirement. To generate the required yaw moment at minimum power, $\Omega_{AY} = \Omega_Y$. Thus, the speed change on the outer perimeter rotors is the same as that on the inner perimeter rotors, as was the case for generation of lift. This is reasonable since the net yaw moment comes from the sum of the individual rotor torques which does not depend on rotor position.

From the above discussions on the hexacopter and the octocopter, extrapolations can be made to the decacopter (Fig. 5). To generate a required thrust at minimum power, $\Omega_0 = \Omega_{A0} = \Omega'_{A0}$, corresponding to equal lift share among all rotors. For pitch and roll moment generation, the rotors 9 and 10 play no role, and the RPM change on the outer perimeter rotors (5-8) is twice that on the inner perimeter rotors (1-4). Or in general, $\Omega_{AP} = \alpha\Omega_P$ and $\Omega_{AR} = \alpha\Omega_R$. For yaw moment generation at minimum power, rotors 9 and 10 again play no role, and the RPM changes on the inner (1-4) and outer (5-8) perimeter rotors is the same, $\Omega_{AY} = \Omega_Y$.

USEFUL WEIGHT, POWER REQUIREMENT AND ENDURANCE COMPARISONS

The empty weight of the various configurations, assessed from the contributions of the hub, booms, motors and rotors is presented in Table 2. Based on the assumption that every rotor/motor combination can generate a maximum thrust of 666.67g in hover, also presented in Table 2 is the maximum gross-weight of each multi-copter configuration. The difference between the maximum gross-weight and the empty weight is used to calculate the maximum useful weight for each configuration. As the number of rotors increases the maximum useful fraction increases from 58.4% for the quadcopter to 73.3% for the decacopter. From Table 2, the maximum useful weight of the octocopter, hexacopter and quadcopter, can be calculated to be 77.3%, 54.6% and 31.9% that of the decacopter.

Table 2: Multi-copter configuration weight comparisons

	Empty Wt (g)	Max GW (g)	Max Useful Wt. (g)	Max Useful Wt (%)
Quadcopter	1108.32	2666.67	1558.35	58.4
Hexacopter	1332.48	4000.00	2667.52	66.7
Octocopter	1556.64	5333.33	3776.69	70.8
Decacopter	1780.80	6666.67	4885.87	73.3

For each multi-copter configuration, the aircraft is trimmed in hover for increments in gross-weight (going from the empty weight to its maximum gross-weight). Minimum power controls are used in each case, and the corresponding power is recorded. Figure 10 shows the power requirement for each multi-copter configuration over its range of useful weight. Instead of reporting the absolute power, the figure presents power normalized with respect to the decacopter's power requirement at the corresponding useful weight. From the figure, it is immediately evident that reconfiguring from the quadcopter up to the decacopter generally reduces power requirement. Consider for example a useful weight of 3.6kg (74% of the decacopter's maximum useful weight). The octocopter consumes about 5.3% more power than the decacopter. At 2.6kg useful weight (53% of the decacopter's maximum useful weight), the octocopter

requires 3.8% more power and the hexacopter requires 6.6% more power than the decacopter. At a useful weight of around 1.55kg (32% of the decacopter's maximum useful weight), the power requirement of the hexacopter and octocopter are comparable to the decacopter, but the quadcopter would require about 8.9% greater power. The improvement in performance with an increasing number of rotors at increasing useful weights is attributed to both a reduction in induced power due to a reduced disk loading, as well as a reduction in profile power due to reduced individual rotor speeds.

At very low useful weights Fig. 10 indicates a steep penalty associated with the use of the larger configurations, with power savings of over 20% seen for the quadcopter and hexacopter (over the decacopter). This penalty for the larger configurations in that useful weight range is attributed to their larger empty-weight fractions. However, it is worth noting that at the lowest useful weights the aircraft is doing very little useful work as it can neither carry a significant payload nor offer significant range/endurance capability due to low battery weight. Considering that a quadcopter or a hexacopter with empty-weight values shown in Table 2 could easily have a useful weight (battery plus payload) in excess of 0.6-0.7kg, the maximum power savings over the decacopter would more likely be capped around 10%. It should be noted that the lower-than-expected power penalty associated with the use of a large airframe (such as a decacopter) at low useful weights is because the penalty associated with the larger empty weight is negated in part by the improved rotor efficiency due to reduced rotor disk loading and rotor operational speeds.

Considering a minimum useful weight constraint of around 0.5kg on Fig. 10, it could be argued that there is no real benefit to using a quadcopter at all. Similarly, there does not appear to be any region where the octocopter power is a minimum. The hover results in Fig. 10 suggest that the hexacopter be used in the 0.5-1.5kg useful weight range, and then reconfigured directly to a decacopter for higher useful weight requirements. This simply requires transitioning back and forth between the configurations in Figs. 2 and 5, by appending or removing rotors at the ends of the quad booms.

Results similar to those in Fig. 10 are shown in Fig. 11 at a forward flight speed of 10 m/s. At these high-speed flight conditions the decacopter does even better. At a useful weight of 3.6kg (74% of the decacopter's maximum useful weight) the octocopter consumes about 8% more power than the decacopter. At 2.6kg useful weight (53% of the decacopter's maximum useful weight), the octocopter requires 6.6% more power and the hexacopter requires 13.4% more power than the decacopter. At a useful weight of 1.55kg (32% of the decacopter's maximum useful weight), the octocopter requires 4.3% more power, the hexacopter requires 7%, and the quadcopter requires around 22.9% more power, compared to the decacopter.

While the results in Figs. 10 and 11 were normalized to the decacopter's power, Fig. 12 shows the actual power (in watts) for the decacopter as a function of useful weight, for both hover and forward flight conditions.

Figure 13 compares the maximum hover endurance (normalized by the battery energy density in kJ/kg) for the various multi-copter configurations, as a function of battery weight (with the assumption that all useful weight is battery weight). For low battery weight of 1/3kg, the endurance of the quadcopter is 20% larger than the decacopter. Here, the larger empty weight of the decacopter (1.78kg compared to 1.11kg for the quadcopter) is a significant contributor to its poorer performance. At a battery weight of 2.6kg, however (corresponding to 53% of the decacopter's maximum useful weight), the endurance of the decacopter is 8..9% higher than that of the hexacopter, with the improved rotor efficiency trumping the higher empty weight. For the decacopter, octocopter and hexacopter, the maximum hover endurance on Fig. 13 is seen to first increase with increasing battery weight, slowly reach a maximum value, and then start to slowly decrease. In essence, for any one of these multi-copters, there comes a point when there is too much battery on board, and the cost of lifting that battery is greater than the benefit. Another way of thinking about it is there is not enough rotor to lift all the battery being placed on board. This idea is supported by the observation that the maximum occurs at progressively higher battery weight as the number of rotors increases.

Table 3: Multi-copter configuration useful weight fraction comparisons

	Battery Wt (kg)	Battery + Empty Wt (kg)	Useful Weight Fraction
Hexacopter	2.2	3.53	0.62
Octocopter	2.5	4.06	0.62
Decacopter	3.1	4.88	0.63

Corresponding to the maximum endurance for the decacopter, octocopter and hexacopter in Fig. 13, Table 3 presents the useful-weight fraction (ratio of battery weight to total aircraft gross weight) for each of the three configurations. The useful weight fraction is seen to be between 0.62-0.63 in each case, suggesting that a useful weight of just over 60% (and a bare airframe weight of under 40%) may be an optimal distribution for multi-copters, at least from a hover endurance capability standpoint. In the case of the quadcopter, the four rotors did not have sufficient lifting capability to overcome the aircraft's empty weight and pack in the battery needed for optimal endurance time (as evident from the quadcopter curve in Fig. 13 truncated by rotor lifting capability before reaching its maxima).

Returning to Fig. 10, the decacopter is seen to be an inferior performer in hover to the hexacopter when the useful weight is less than 1.5kg, or around 30% of its maximum useful

weight. Thus, for the decacopter, in addition to noting that the maximum useful weight is 73% (Table 2) and the optimum battery weight for maximum hover time is 63%, when the useful weight is less than 30% of the maximum useful weight, the penalty of the larger airframe weight dominates, and the decacopter would not be the configuration of choice.

CONTROL AUTHORITY COMPARISONS

The ability of the multi-copter to generate pitch, roll or yaw moments, and accelerations, has direct implications on the aircraft handling qualities and agility. For this analysis, recall that each rotor is assumed to have a minimum operational speed of 2,000 RPM and a maximum operational speed of close to 8,000 RPM. In hover condition, Fig. 14 shows a comparison of the maximum pitching moment that can be introduced on the multi-copter configurations as a function of useful weight. In general, the maximum pitching moment on the octocopter and the decacopter is considerably larger than that on the quadcopter and hexacopter. Figures 15, 16, 17 and 18, respectively, present the individual rotor speeds on the quadcopter, hexacopter, octocopter and decacopter that generate the maximum nose-down pitching moments seen on Fig. 14. For the quadcopter, maximum pitching moment corresponding to the empty weight of the aircraft has the front rotors spinning at minimum RPM. As the useful weight increases, the rear rotors speed up (Fig. 15), and the pitching moment increases, until the rear rotors reach their maximum speed (at 0.5kg useful weight). Further increase in useful weight requires the front rotors to progressively speed up (Fig. 15) until they reach their maximum speed. But the speeding up of the front rotors (while the rear rotors are at maximum speed) reduces the maximum pitching moment that can be generated, as seen on Fig. 14.

Comparing the individual rotor speeds on the hexacopter (Fig. 16) to the quadcopter (Fig. 15), it is observed that after the rear rotors have reached their maximum speed, further increase in useful weight has the middle rotors (5 and 6, on Fig. 2) speeding up to provide more lift. Since the front rotors stay at the minimum speed, the maximum pitching moment holds (as seen in the flat part of the hexacopter curve on Fig. 14), until the middle rotors (5 and 6) have reached their maximum speed. Further increase in useful weight (beyond 1.6kg) requires the front rotors to speed up and the maximum pitching moment reduces, as was the case with the quadcopter.

Figure 17 shows the individual rotor speeds for the octocopter. To generate maximum nose-down pitching moment corresponding to the aircraft empty weight puts all the rotors at minimum speed, except for the rear rotors (7 and 8 on Fig. 4) at close to maximum speed. With increasing useful weight, these rear rotors would speed up first. As soon as they reach their maximum speed, the mid-rear rotors (3 and 4 on Fig. 4) start to speed up, until they reach their maximum speed. Further increase in useful weight requires the mid-front rotors (1 and 2 on Fig. 4) to speed up, but this starts to reduce the maximum nose-down pitching moment that can be generated, as seen on Fig. 14. Once the mid-front rotors reach their maximum speed, further increase in useful weight has the front-most rotors (5 and 6 on Fig. 4) speeding up, and further reducing the maximum pitching moment capability.

Figure 18 shows the individual rotor speeds for the decacopter. The results are generally similar to the octocopter results, except that once the mid-rear rotors have reached their maximum speed the middle rotors (9 and 10 on Fig. 5) start to speed up. The mid-front rotors (1 and 2 on Fig. 5) speed up only after the middle rotors have reached their maximum speed. As was the case for the hexacopter, this produces a plateau on the maximum pitching moment graph for the decacopter, as seen on Fig. 14.

Figure 19 presents the maximum pitch accelerations that can be generated on the various multi-copter configurations. In addition to the pitching moments (Fig. 14) the pitch inertia of the various configurations is a factor. As seen on Fig. 19, the quadcopter and hexacopter produce larger maximum pitching accelerations in the low useful weight range due to their significantly lower pitch inertia. At higher useful weights, though, their ability to produce pitch accelerations is reduced due to the rotors operating close to capacity and thus being unable to generate large moments. The maximum pitch acceleration produced by the quadcopter or hexacopter at lower useful weights of 1.55kg (32% of the decacopter's maximum useful weight) is about 78% higher than that the octocopter or decacopter can produce. But at 2.6kg (53% of the decacopter's maximum useful weight) the hexacopter's maximum pitch accelerations are 60% lower than the decacopter's.

A similar analysis was conducted on the generation of maximum roll moments and maximum roll accelerations on the various multi-copter configurations in hover, and the results were similar to those seen for pitch. Once again, the octocopter and decacopter produced larger moments, but lower maximum roll accelerations due to their higher roll inertia (relative to the quadcopter and hexacopter).

Lastly, the various multi-copter configurations are compared in terms of their ability to generate a maximum yaw moment (Fig. 20) and maximum yaw acceleration (Fig. 21). Figures 22 and 23 show the individual rotor speeds for the octocopter and decacopter (corresponding to the results in Figs. 20 and 21). To generate a maximum nose-right yaw moment at the aircraft empty weight, the clockwise rotors operate at their minimum speed. As the aircraft useful weight increases, the counter-clockwise rotors speed up to produce larger nose-right moments, until they reach their maximum speed. In the case of the octocopter, further increase in useful weight requires the clockwise rotors to speed up (Fig. 22), which reduces the maximum nose-right yaw moment that can be produced. In the case of the

decacopter, the middle rotors (9 and 10 on Fig. 5) speed up before the clockwise rotors do (Fig. 23). Because these rotors, as a pair, are yaw-neutral even as they support an increase in useful weight, a plateau is observed on Fig. 20 for the decacopter. A similar plateau is observed for the hexacopter when the middle rotors (5 and 6 on Fig. 2) are speeding up. It is interesting to note on Fig. 23 that the increase in RPM of the middle rotors is much faster (for a given increase in useful weight) than the increase rise seen first for the counter-clockwise rotors and later for the clockwise rotors. This is because there are four counter-clockwise or clockwise rotors speeding up, while there are only two middle rotors. Although the maximum yaw-moments generated by the octocopter and decacopter are larger than the quadcopter and hexacopter, their larger yaw inertias result in lower maximum yaw accelerations (Fig. 21). At a useful weight of around 1.55kg (32% of the decacopter's maximum useful weight), the maximum yaw acceleration of a hexacopter is about 94.5% greater than that of the decacopter. At a useful weight of 2.55kg (53% of the decacopter's maximum useful weight), however, the maximum yaw acceleration of the hexacopter is 56.5% lower than the decacopter.

AUTONOMOUS FLIGHT DYNAMICS

In Ref. 8, the autonomous flight dynamic characteristics of classical quadcopters (with evenly spaced rotors) were discussed in detail. In hover, such quadcopters were reported to exhibit two oscillatory modes, a longitudinal and a lateral phugoid mode, with both modes being stable and their poles coincident. The longitudinal phugoid mode combined longitudinal translation (surge) with pitch motion, while the lateral phugoid mode coupled lateral translation (sway) with roll. The dominant contributor to the damping in the longitudinal phugoid mode was the increasing downwash on the front rotor(s) reducing their thrust when the aircraft had a nose-up pitch rate, and conversely, the increasing upwash on the rear rotor(s) increasing their thrust. A similar stabilizing mechanism was observed in the lateral phugoid mode with roll rate generating upwash/downwash on the left/right rotors.

In the present study, all the multi-copter configurations displayed the longitudinal and lateral phugoid modes in hover. However, considerable differences were observed increasing in size from the quadcopter up to the decacopter. Figures 24 and 25 show the longitudinal and lateral phugoid mode frequencies as a function of useful weight, and Figs. 26 and 27 show the corresponding damping ratios. The hexacopter, due to its equal azimuthal spacing of rotors, has its longitudinal and lateral phugoid mode poles coincident (the frequencies are identical on Figs. 24 and 25, as are the damping ratios on Figs. 26 and 27). The frequencies of the longitudinal phugoid modes for the octocopter and decacopter are substantially lower than the quadcopter and hexacopter (Fig. 24) due to their significantly larger pitch inertias. On the other hand, the lateral phugoid mode frequencies progressively decrease (Fig. 25) as the roll inertia progressively increases going from the quadcopter to the hexacopter to the octocopter to the decacopter.

The damping mechanism explained in the first paragraph of this section associated with pitch rate or roll rate inducing upwash/downwash on specific rotors is strengthened when the rotors have a higher disk loading. Thus, it is observed on Figs. 26 and 27 that the phugoid mode damping generally increases with increasing useful weight. On Fig. 26, this is also the reason why the hexacopter has a lower longitudinal phugoid mode damping ratio than the quadcopter (whose rotors have a higher disk loading at comparable weights). A similar explanation holds for the decacopter having lower damping ratio than the octocopter. Comparing the two larger aircraft (octocopter and decacopter) to the two smaller aircraft (quadcopter and hexacopter), the higher pitch inertia of the larger aircraft appear to be more destabilizing than the increased aerodynamic damping of additional rotors with larger moment arms. Similarly, in Fig. 27, the octocopter and decacopter lateral phugoid mode damping is lower than the hexacopter's damping due to the higher roll inertia and the lower disk loading being more influential than the larger stabilizing aerodynamic moments due to rotors farther out laterally. Comparing the hexacopter to the decacopter at a gross-weight of 2.6kg (53% of the decacopter's maximum useful weight), the damping in the longitudinal and lateral phugoid modes is 20% and 39% less for the decacopter.

Finally, Figs. 28 and 29 examine the longitudinal and lateral phugoid mode shapes for the various configurations. Specifically, Fig. 28 presents the ratio of the magnitude of the surge velocity to pitch rate in the longitudinal phugoid mode. It is evident that the larger configurations (octocopter and decacopter) have a significantly higher surge component in their longitudinal phugoid modes. This is attributed to their significantly larger pitch inertia. For the lateral phugoid mode, Fig. 29 shows a more progressive increase in the ratio of sway velocity to roll rate as the multi-copter configuration grows from the quadcopter to the decacopter. This is related to the progressive increase in roll inertia. In contrast, the pitch inertia did not increase going from the quadcopter to the hexacopter, or from the octocopter to the decacopter in Fig. 28.

CONCLUSIONS

This paper presents a concept of a multi-copter that can be reconfigured between a quadcopter, hexacopter, octocopter and decacopter. The maximum useful weights of the octocopter, hexacopter and quadcopter, were 77%, 55% and 32% that of the decacopter. The controls for each of the configurations are identified and for the configurations that have control redundancies the power optimal controls are presented. A dynamic simulation model is implemented using blade-element theory coupled with Peters-He dynamic wake model to calculate the rotor aerodynamic forces and moments, and the performance of the various configurations is compared. From the results presented in the paper the following conclusions were drawn:

The power requirements of the decacopter were compared to the other configurations in both hover and at 10m/s forward flight speed. When the decacopter is operating at 74% of its maximum useful weight, the octocopter (which at the same useful weight is operating close to its maximum) requires 5.3% more power in hover and 8% at 10 m/s forward speed. When the decacopter is operating at 53% of its maximum useful weight, the hexacopter (which at the same useful weight is operating close to its maximum) requires 6.6% more power in hover and 13.4% at 10 m/s forward speed. The octocopter, at the same useful weight requires 3.8% more power in hover and 6.6% at 10 m/s forward speed. When the decacopter is operating at 32% of its maximum useful weight, the quadcopter (which at the same useful weight is operating at just about its maximum) requires 8.9% more power in hover and 22.9% at 10 m/s forward speed. At the same useful weight, the power requirements of the hexacopter and octocopter are comparable to the decacopter in hover, but 7% and 4.3% higher at 10m/s forward flight speed.

The lower power requirement of the decacopter, when the useful weight is greater than around 30% of its maximum, is attributed to the improved rotor efficiency. Both the induced power as well as the profile power reduce; the former due to reduced disk loading and the latter due to lower rotational speed. When the useful load decreases below around 30% of the decacopter's maximum, the hexacopter offers power reductions in the range of around 10% in hover and 5% in forward flight. The reduced performance of the decacopter is attributed to its significantly larger empty weight (and therefore high empty weight fraction at low useful weights), relative to the hexacopter. Notably, for the rotors used as the building blocks for the multi-copters in this paper, the octocopter and quadcopter do not emerge as high-performers. The results suggest that from a power requirement perspective, if the useful load is greater than about 30% of the decacopter's maximum useful load, the decacopter will have the lowest power requirement. For lower useful loads the hexacopter emerges as the low-power configuration of choice.

Hover endurance: In general, increasing the number of rotors increased the maximum hover endurance because the larger aircraft could carry more battery, and at given battery weight, a larger number of rotors resulted in greater rotor efficiency. At a useful weight corresponding to 53% of the decacopter's maximum useful weight, the decacopter's hover endurance time was 8.9% higher than that of the hexacopter. For the hexacopter, octocopter and decacopter, the maximum hover endurance condition corresponded to that aircraft having a battery weight fraction of just above 60%.

Control Authority: In hover, although the maximum pitch, roll and yaw moments generated by the smaller multi-copters (quadcopter and hexacopter) are significantly lower than those generated by the octocopter and decacopter, the lower inertias resulted in larger accelerations at low useful weights. At higher useful weights though, the smaller multi-copters were required to speed up most of the rotors, and the ability to generate large moments (and accelerations) by maximizing the speed differences between rotors was diminished. The results showed that at 32% of the decacopter's maximum useful weight, the maximum pitch and yaw accelerations of the hexacopter were 78% and 94.5% higher than the decacopter's, but at 53% of the decacopter's maximum useful weight, these accelerations were 60% and 56.5% lower than the decacopter's.

Autonomous Flight Dynamic Characteristics: All multi-copter configurations displayed a longitudinal and lateral phugoid mode in hover. Due to their lower inertia, the smaller configurations displayed higher phugoid mode frequencies. The phugoid mode shapes for the larger configurations had significantly higher components of surge rate compared to pitch rate, or sway rate compared to roll rate, than the modes for the smaller configurations. The damping in the phugoid modes increased with increasing useful weight for all configurations, and was generally higher for the smaller configurations. At a useful weight of 53% of the decacopter's maximum, the damping in the hexacopter's longitudinal and lateral phugoid modes was 20% and 39% higher than the decacopter's.

Author contact: Robert Niemiec 1 niemir@rpi.edu,
Farhan Gandhi fgandhi@rpi.edu,
Rajneesh Singh rajneesh.k.singh.civ@mail.mil.

ACKNOWLEDGMENTS

The authors acknowledge the contribution of Mr. Michael Juan, undergraduate research assistant at RPI, in generating some of the simulation results.

REFERENCES

1. Rothhar, P., Murphy, P., Bacon, B., Gregory, I., Grauer, J., Busan, R., and Croom, M., *NASA Langley Distributed Propulsion VTOL Tilt-Wing Aircraft Testing, Modeling, Simulation, Control, and Flight Test Development*, 14th AIAA Aviation Technology, Integration, and Operations Conference, Atlanta, GA, June 16-20, 2014.
2. Stoll, A., Bevirt, J., Pei, P., and Stilson, E., *Conceptual Design of the Joby S2 Electric VTOL PAV*, 14th AIAA Aviation Technology, Integration, and Operations Conference, Atlanta, GA, June 16-20, 2014.
3. Stoll, A., Bevirt, J., Moore, M., Fredericks, W., and Borer, N., *Drag Reduction Through Distributed Electric Propulsion*, 14th AIAA Aviation Technology, Integration, and Operations Conference, Atlanta, GA, June 16-20, 2014.
4. AHS Staff, "Lightning Strikes Aurora: DARPA Awards VTOL X-Plane Demonstrator Contract," *Vertiflite*, May-June 2016, pp. 10-11.
5. Whittle, R., "The Demand for On-Demand Mobility," *Vertiflite*, January-February 2017, pp. 34-38.

6. Whittle, R., "Air Mobility Bonanza Beckons Electric VTOL Developers," *Vertiflite*, March-April 2017, pp. 14-21.
7. Duffy, M., and Samaritano, T., *The LIFT! Project -- Modular, Electric Vertical Lift System*, 71st Annual Forum of the American Helicopter Society, Virginia Beach, VA, May 5-7, 2015.
8. Niemiec, R., Gandhi, F., *A Comparison Between Quadrotor Flight Configurations*, 42nd European Rotorcraft Forum, Lille, France, Sept 5-7, 2016.
9. Niemiec, R., Gandhi, F., *Multi-rotor Coordinate Transforms for Orthogonal Primary and Redundant Control Modes for Regular Hexacopters and Octocopters*, 42nd European Rotorcraft Forum, Lille, France, Sept 5-7, 2016
10. Peters, D., He, C., *A finite-state induced-flow model for rotors in hover and forward flight*, 43rd Annual National Forum of the American Helicopter Society, St. Louis, MO, May 1987.

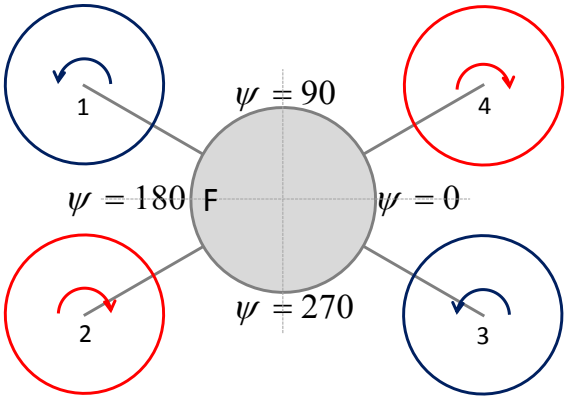

Fig. 1: Baseline quadcopter

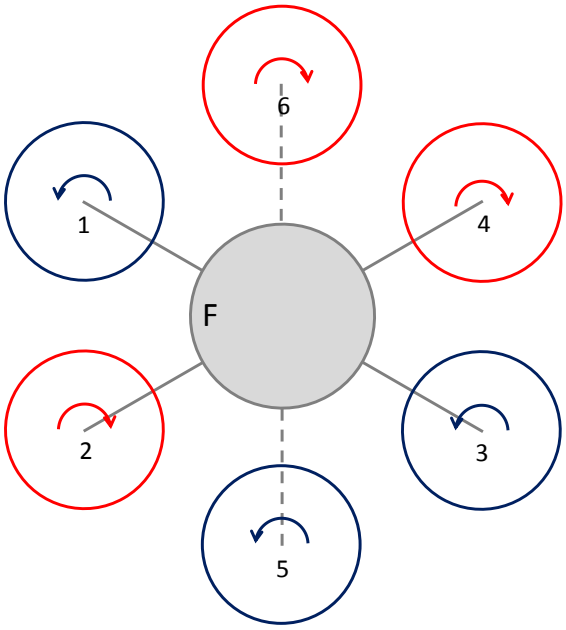

Fig. 2: Quadcopter extended to hexacopter

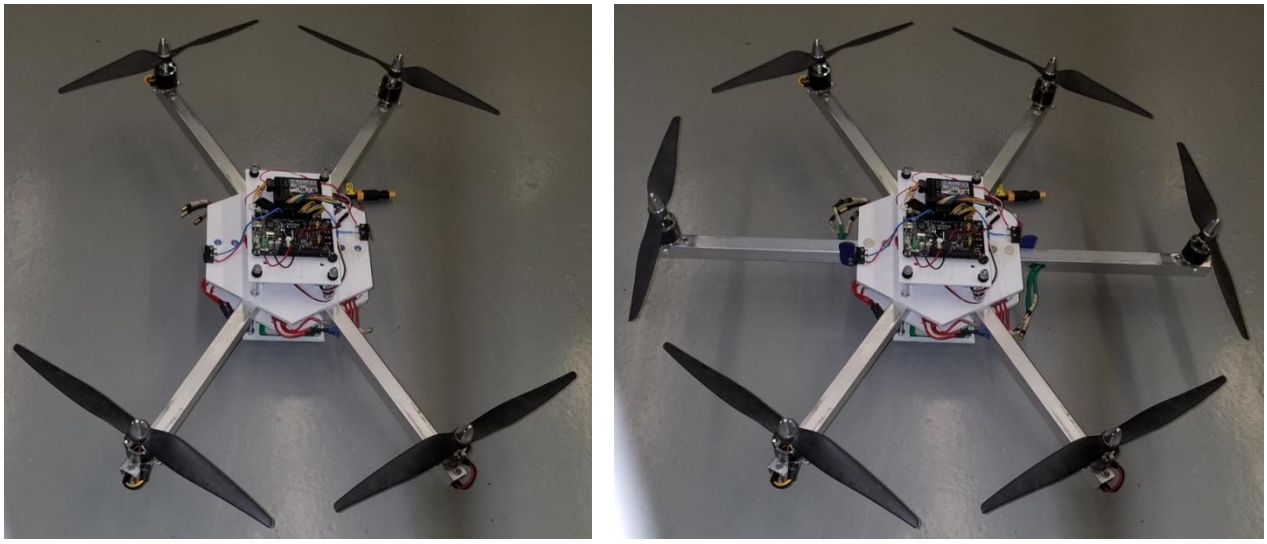

Fig. 3: Hardware of reconfigurable multi-copter showing quadcopter (left) extended to hexacopter (right)

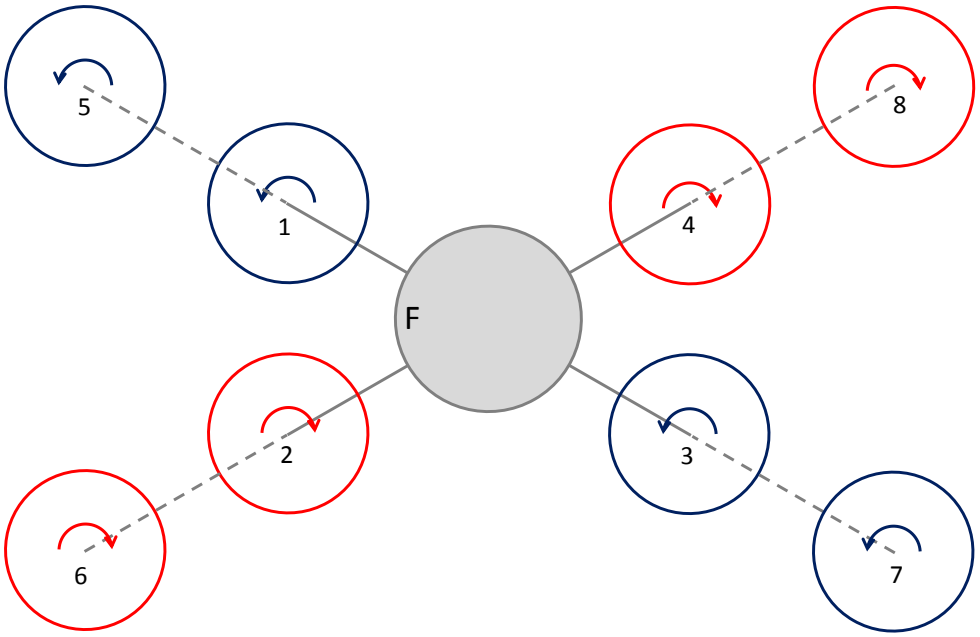

Fig. 4: Extended boom octocopter

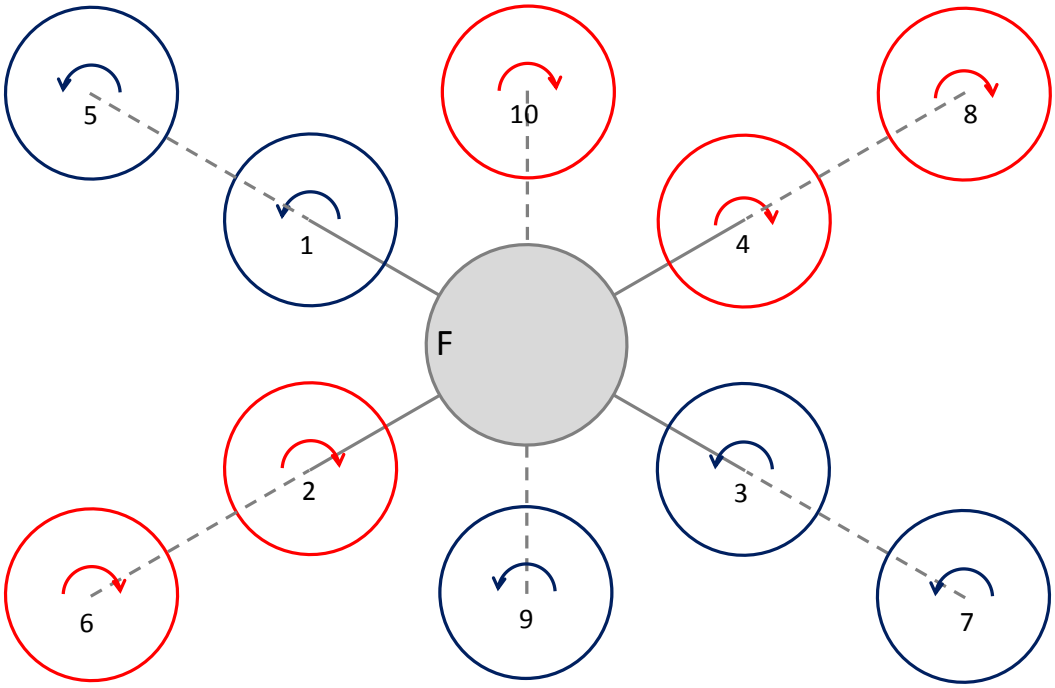

Fig. 5: Decacopter

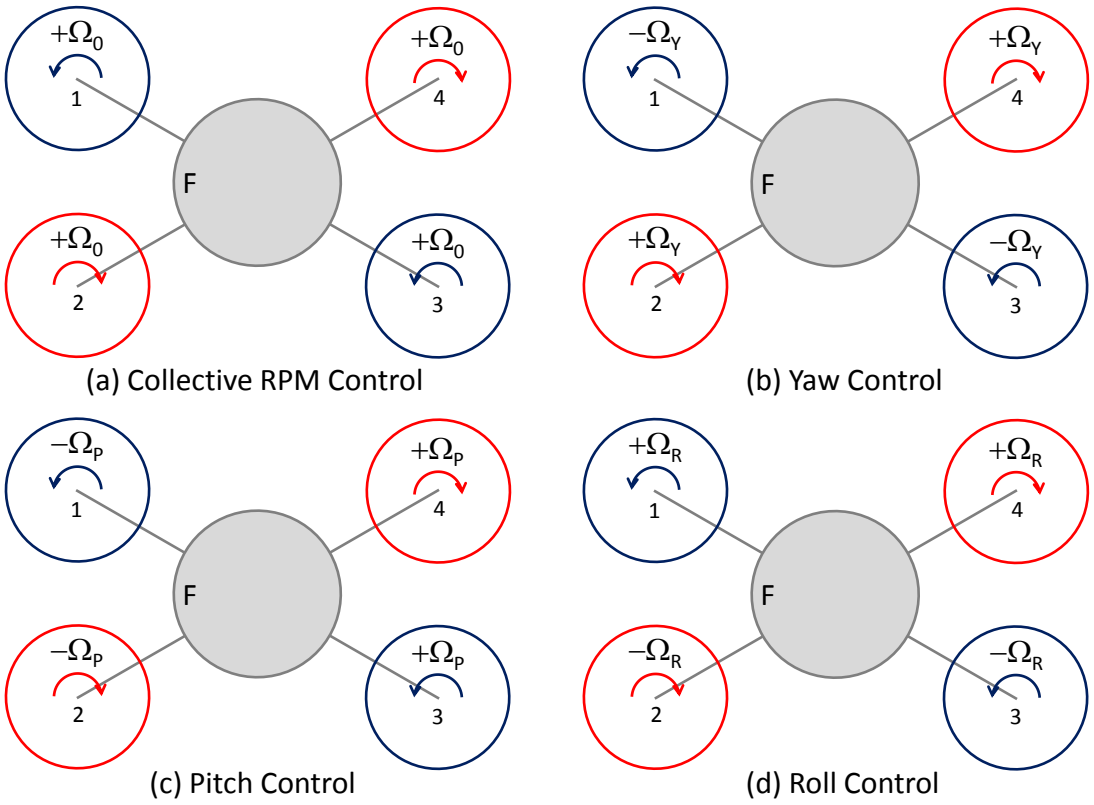

Fig. 6: Quadcopter multi-rotor controls

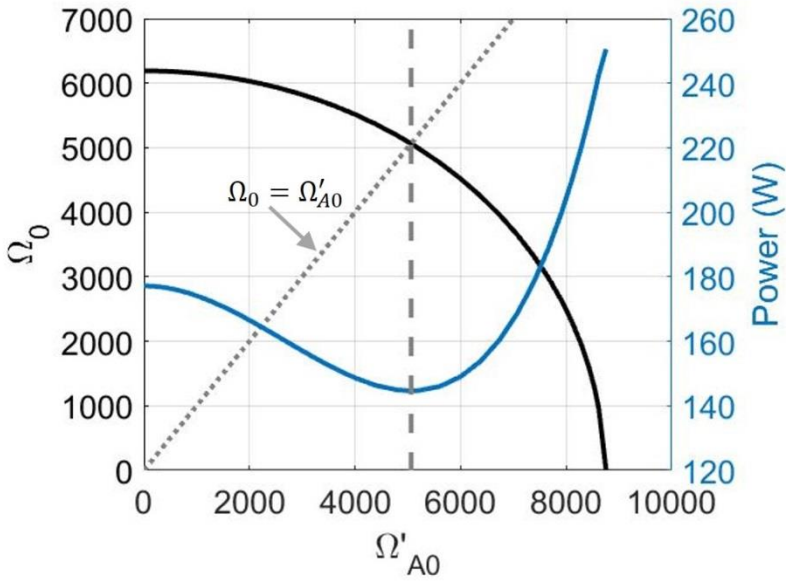

Fig. 7: Hexacopter collective RPM control and power required, versus redundant control, Ω'_{A0}

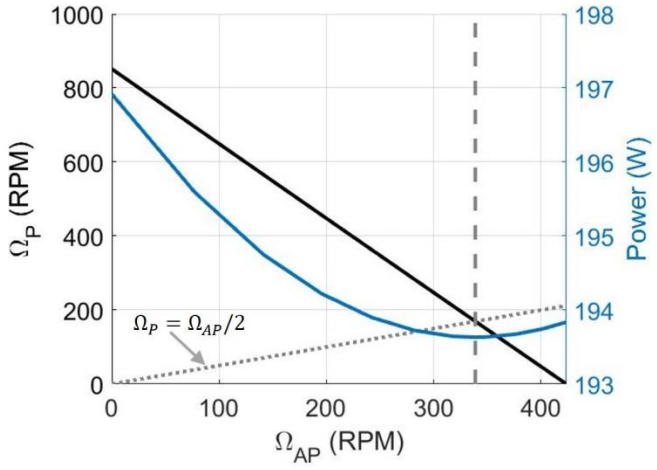

Fig. 8: Octocopter pitch control and power required, versus auxiliary pitch control, Ω_{AP}

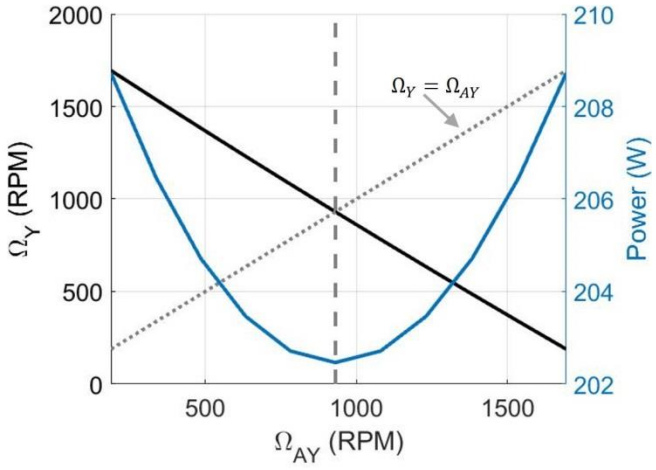

Fig. 9: Octocopter yaw control and power required, versus auxiliary yaw control, Ω_{AY}

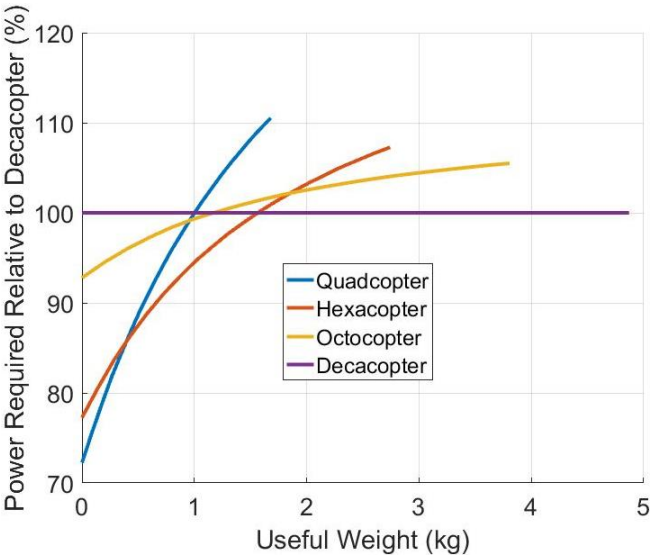

Fig. 10: Multi-copter power requirements in hover

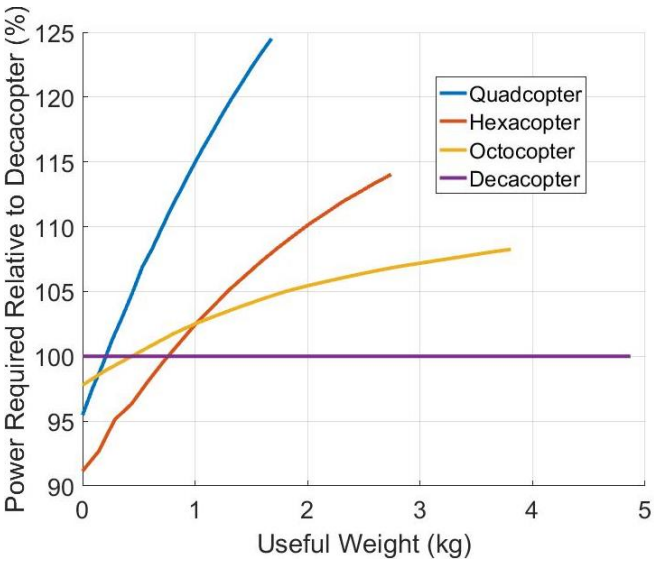

Fig. 11: Multi-copter power requirements at 10m/s

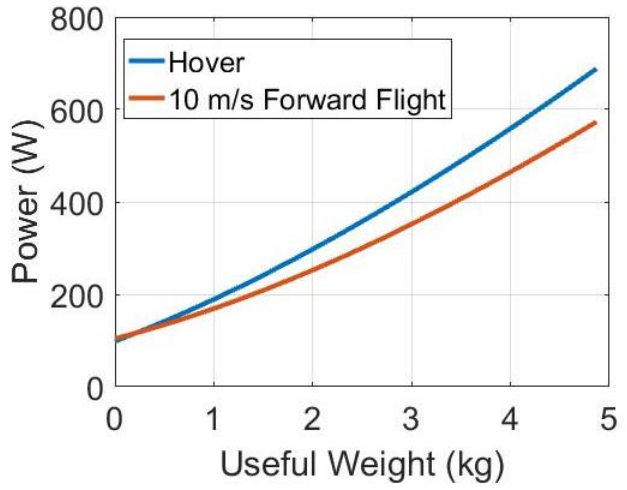

Fig. 12: Decacopter power in hover and at 10m/s

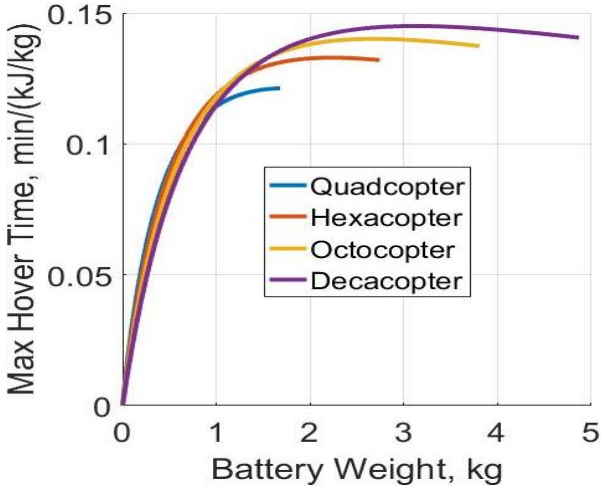

Fig. 13: Max over endurance of various configurations

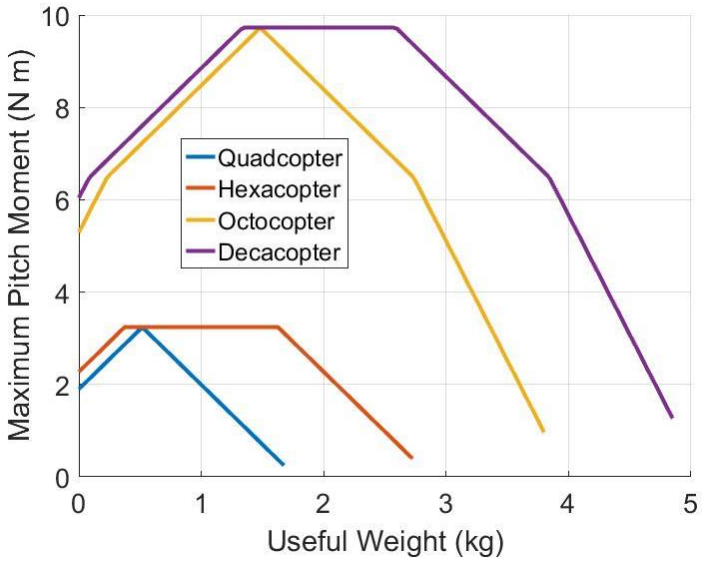

Fig. 14: Maximum pitching moment for the various multi-copter configurations

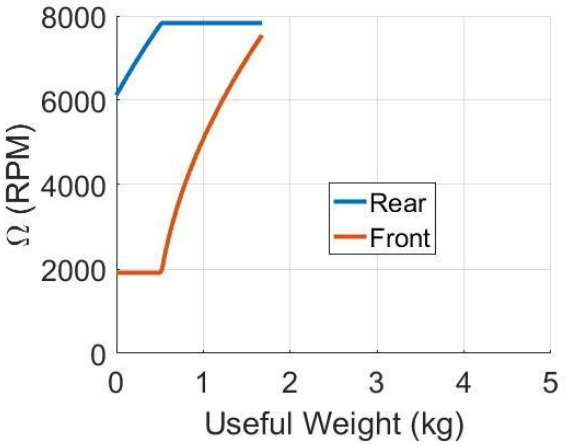

Fig. 15: Quadcopter controls for max pitching moment

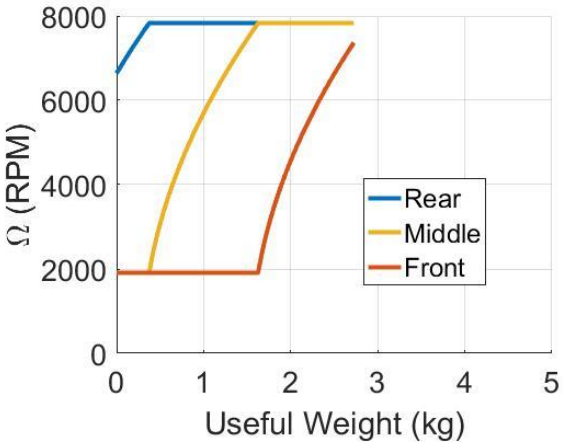

Fig. 16: Hexacopter controls for max pitching moment

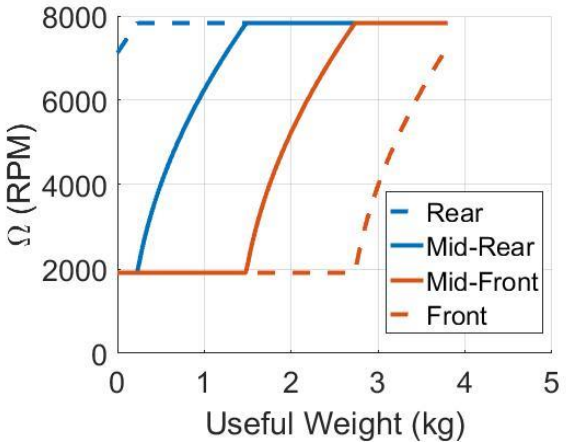

Fig. 17: Octocopter controls for max pitching moment

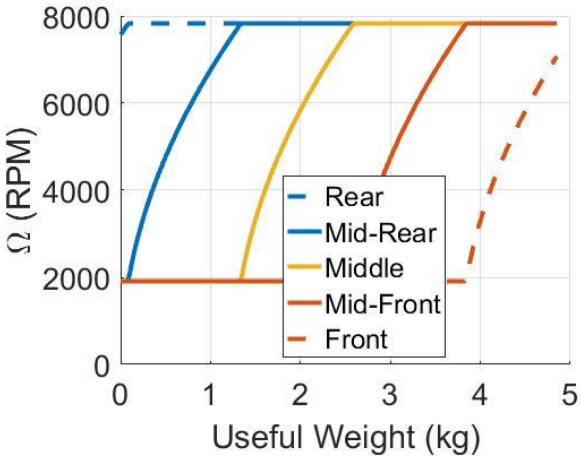

Fig. 18: Decacopter controls for max pitching moment

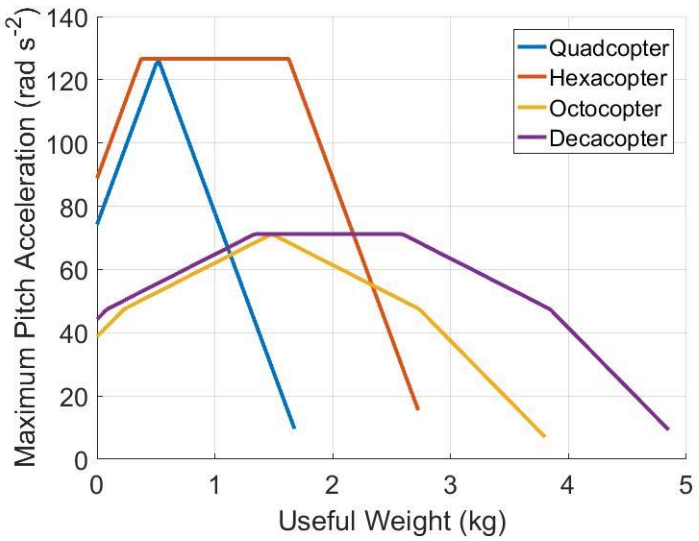

Fig. 19: Maximum pitching accelerations for the various multi-copter configurations

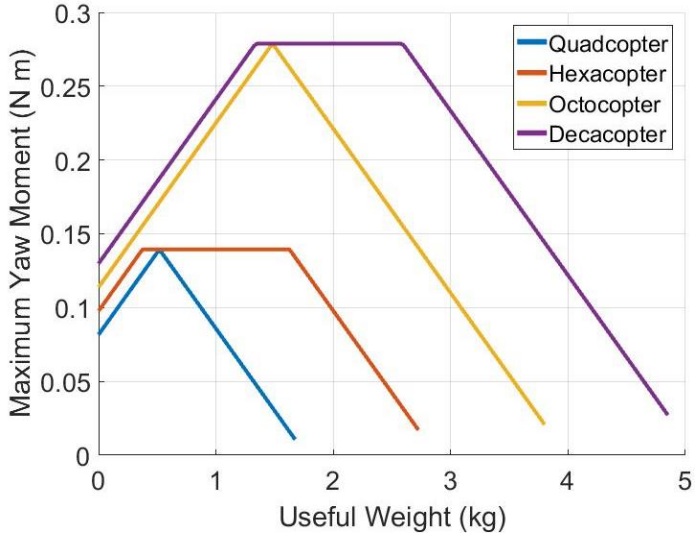

Fig. 20: Maximum yaw moment for the various multi-copter configurations

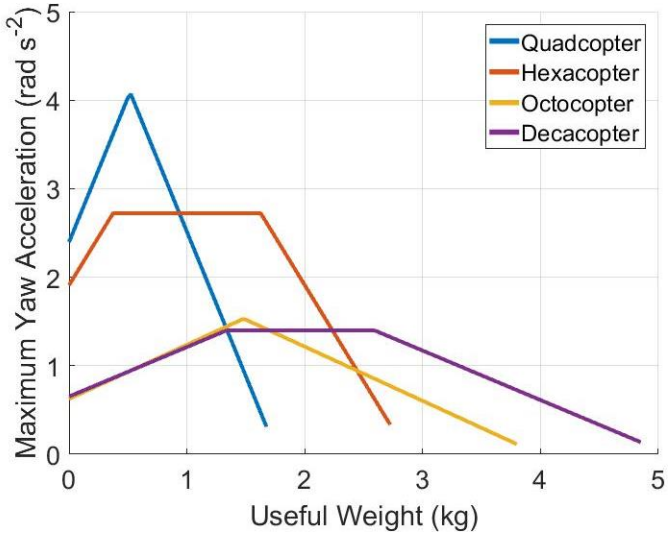

Fig. 21: Maximum yaw accelerations for the various multi-copter configurations

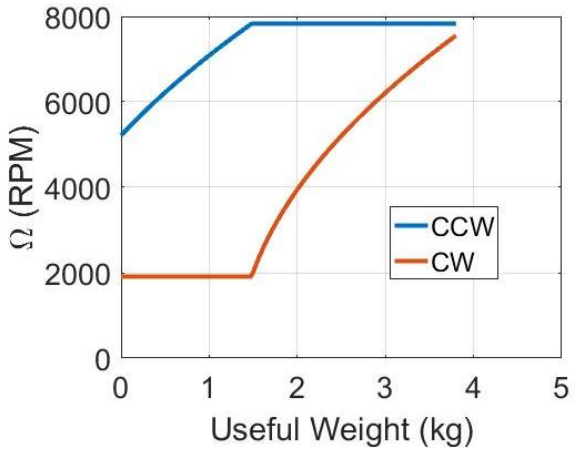

Fig. 22: Octocopter controls for max yaw moment

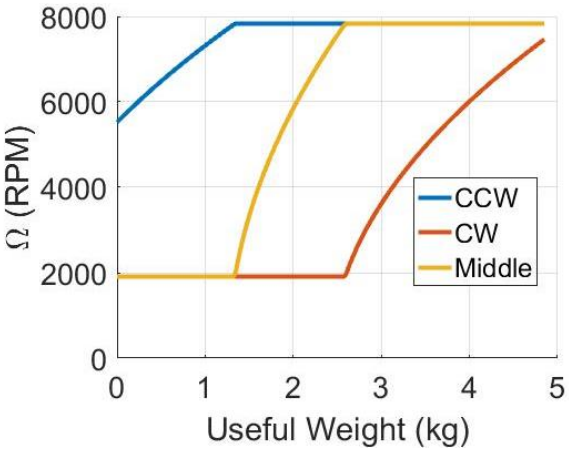

Fig. 23: Decacopter controls for max yaw moment

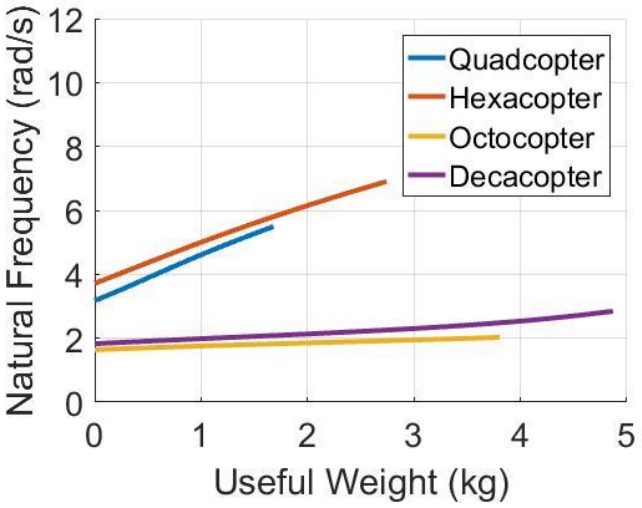

Fig. 24: Longitudinal Phugoid Mode Frequency

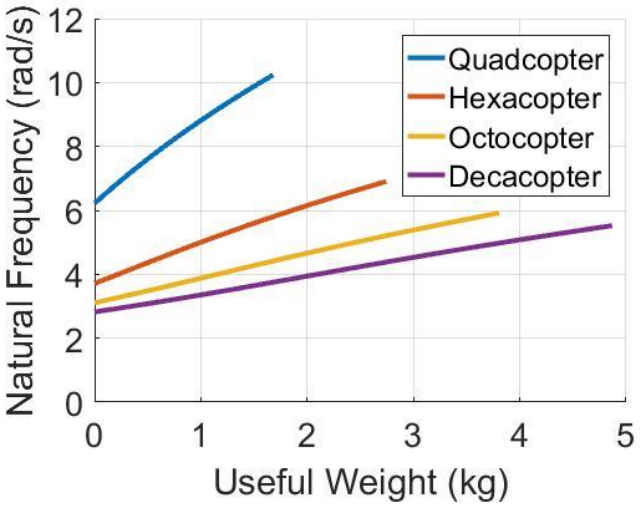

Fig. 25: Lateral Phugoid Mode Frequency

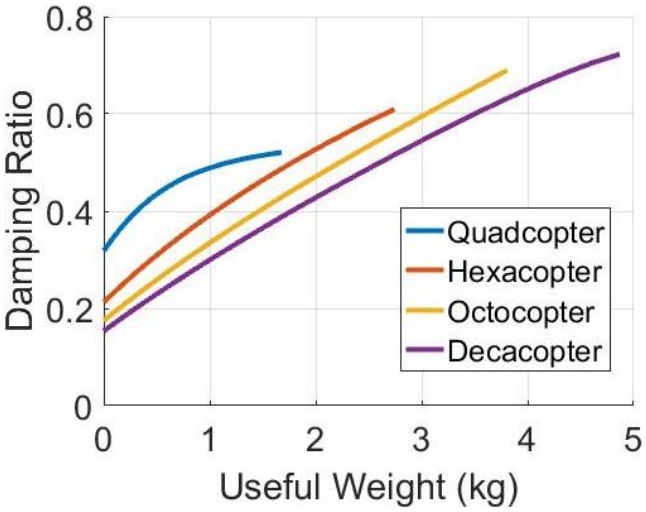

Fig. 26: Longitudinal Phugoid Mode Damping

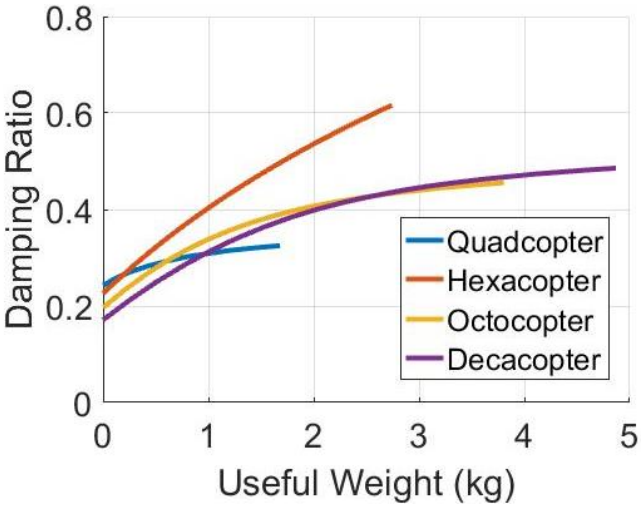

Fig. 27: Lateral Phugoid Mode Damping

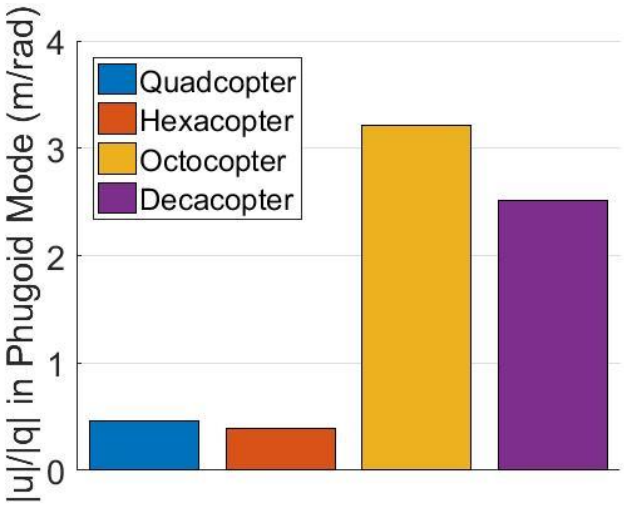

Fig. 28: Longitudinal Phugoid Mode Shape

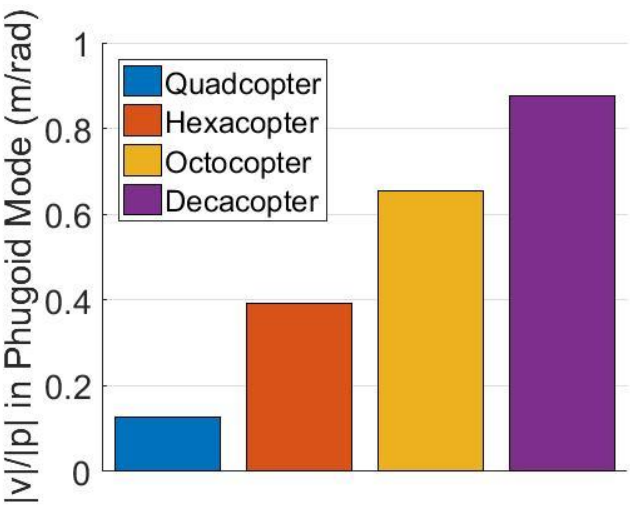

Fig. 29: Lateral Phugoid Mode Shape